

# The influence of iron content on the promotion of the zircon structure and the optical properties of pink coral pigments

Giuseppe Cappelletti<sup>a</sup>, Silvia Ardizzone<sup>a,\*</sup>, Paola Fermo<sup>b</sup>, Stefania Gilardoni<sup>b</sup>

<sup>a</sup> Department of Physical Chemistry and Electrochemistry, University of Milan, Via Golgi 19, 20133 Milan, Italy

<sup>b</sup> Department of Inorganic, Metallorganic and Analytical Chemistry, University of Milan, Via Venezian 21, 20133 Milan, Italy

Received 4 February 2004; received in revised form 2 April 2004; accepted 22 April 2004

Available online 2 July 2004

## Abstract

A sol–gel reaction starting from Si and Zr alkoxides, in water-ethanol mixtures, was employed to obtain iron doped zirconium silicate powders (zircon). The starting amount of the ferric salt in the sol–gel reacting mixture was varied in order to obtain  $\text{Fe}_2\text{O}_3/\text{Zr}$  molar ratios in the range 0.7–10%. The products of the sol–gel reaction were calcined in the range 800–1300 °C. X-ray diffractograms, EDX analyses and diffuse reflectance spectra were obtained and analysed for all the calcined powders; the colour of the pigments was characterised on the grounds of the CIE (Commission Internationale de l’Eclairage) standard procedure (CIE  $L^*a^*b^*$  measurements). Results from the structural and spectral characterisations are examined and cross-compared to produce a consistent picture of the role played by iron on the promotion of the zircon lattice and on the optical properties of the reaction products.

© 2004 Elsevier Ltd. All rights reserved.

**Keywords:** Pink coral; Zircon; Pigments; Sol–gel processes; Optical properties; X-ray methods

## 1. Introduction

Zircon,  $\text{ZrSiO}_4$ , assumes a garnet-like structure in which guest metal ions can be incorporated to give coloured materials. The metal dopant can be accommodated into the zircon network as a guest cationic species, either interstitial or substitutional, or be present as a separate oxide phase. In several cases controversial conclusions are reached in the literature concerning the actual location of the metal and its valence in the zircon lattice.<sup>1–13</sup>

The doping of the zirconium silicate matrix by iron provokes the formation of a coral-red material which is one of the most widely used zircon-based pigments.

In the case of iron-doped zircon pigments the valence of the metal, in the host matrix, is generally accepted to be three and this has, also, been directly verified by Mossbauer spectroscopy.<sup>9</sup> The more controversial topics, in this case, concern instead the role played by iron in the formation of the zircon lattice<sup>6,12,13</sup> and the actual presence, in the pigment (i) of iron cations either in interstitial or in substi-

tutional positions, or (ii) of segregated hematite.<sup>6–8,10,11,13</sup> In this latter case debate exists concerning the occurrence of the oxide as a separate phase or encapsulated in the zircon lattice.<sup>10,11,13</sup>

The role played by the metal on the promotion of the zircon lattice is hardly negligible. Several authors suggest that the metal may act as an initiator in the nucleation of the zircon structure within the zirconia lattice.<sup>5</sup> Eppler has shown that during the formation of the zircon pink pigment, silica is transported in a fluid state to reaction sites promoted by iron in the zirconia lattice. The reaction occurs and it is limited at first by the rate at which the zircon product is nucleated and subsequently by the diffusion of silica through the zircon layer.<sup>12,13</sup>

In the case of high iron loading, Tartaj et al.<sup>5</sup> have observed that before the formation of zircon, tetragonal zirconia forms with a unit cell volume smaller than that of the blank, suggesting the formation of a solid solution between the iron cations and the zirconia lattice. The process generates vacancies which favour the nucleation of zircon. The authors<sup>5</sup> suggest that after the zircon formation iron(III) segregates with the ensuing formation of hematite and that hematite is the only responsible of the red colour of the iron zircon pigment. The same authors have observed

\* Corresponding author. Tel.: +39 02 503 14225; fax: +39 02 503 14300.

E-mail address: [silvia.ardizzone@unimi.it](mailto:silvia.ardizzone@unimi.it) (S. Ardizzone).

by XPS that the surface Fe/ZrSiO<sub>4</sub> ratio is comparable to the average iron content of the sample indicating that hematite is homogeneously distributed in the zircon matrix.

Berry et al.,<sup>7,8</sup> in the case of samples prepared by the ceramic method and in the presence of mineralisers, have found that iron is present in the pigment both as hematite and also as Fe<sup>3+</sup> species in interstitial rhombic and axial sites; the effective accommodation of iron in the lattice was found to depend on the final concentration of the dopant in the pigment, and the authors concluded that, for contents higher than 1 mass%, the colour was dominated by hematite inclusions. Gair et al.<sup>2</sup> reported, in their turn, the existence of Fe<sup>3+</sup> cations in the lattice but located in 4-coordinated positions of the zircon lattice substituting for silicon and not in interstitial positions as reported by Berry et al.<sup>8</sup>

The presence in the literature of divergent results concerning various aspects of these systems is, at least in part, due to the manifold features of these materials, and to the close interplay between different parameters introduced by the preparative steps. In fact the adopted preparative route plays, in the present authors opinion, a key role in defining the final features of the pigments. Consistently with these considerations, Monros and co-workers<sup>6</sup> have recently shown that the conditions adopted for the sol–gel process and particularly the sequence of the iron addition to the reacting mixture lead to the formation of samples with different phase composition and colour.

In a recent work performed in our laboratory<sup>14</sup> we have observed that in the case of iron-zircon pigments, obtained by a sol–gel procedure, the speciation of iron and the length of the hydrolysis-condensation steps affected both the bulk and the morphological features of the samples. Further, iron ions were found to be present in the samples both as hematite and also as interstitial ions located in octahedral positions of the zircon lattice. By elaboration of diffuse reflectance spectra both interstitial ions and hematite appeared to contribute to the colour of the pigment.

The present work is aimed at obtaining a better understanding concerning the effects provoked by the variation of the iron concentration with respect to both the zircon lattice promotion and colour of the pigments. A sol–gel preparative route was selected as, with comparison to the classical ceramic preparations, it allows a homogeneous distribution of the guest metal species both in the starting reaction mixture and in the ensuing gel and xerogel. The structural features have been analysed for all the samples as a function of the calcination temperature. Spectral reflectance measurements were performed to obtain information concerning the optical properties of the powders.

## 2. Experimental

All the chemicals were of reagent grade purity and were used without further purification; doubly distilled water

passed through a Milli-Q apparatus was used to prepare solutions and suspensions.

### 2.1. Sample preparation

The zircon samples were prepared by a sol–gel procedure consisting of two different hydrolysis steps. In the reaction, the water/alkoxide (75) and the catalyst alkoxide (0.5) molar ratios were chosen such as to promote a fast hydrolysis step. The occurrence of a fast hydrolysis step, in the sol–gel preparation of an oxide, leads to products with large surface areas; further, in the case of iron doped red pigments, precursors showing larger surface areas have been observed to crystallise more easily to zircon.<sup>14</sup>

At the beginning Si(OC<sub>2</sub>H<sub>5</sub>)<sub>4</sub> (0.20 mol) was added drop by drop to a solution (260 ml) of milli-Q water and iron(III) salt (FeCl<sub>3</sub>·6H<sub>2</sub>O, Fe(NO<sub>3</sub>)<sub>3</sub>, FeSO<sub>4</sub>) at different concentrations in order to have in the end 0.007, 0.02, 0.03, 0.045, 0.05, 0.06, 0.10 Fe<sub>2</sub>O<sub>3</sub>/Zr molar ratios. The mixture was stirred at 60 °C for about 20 min in order to achieve the complete dissolution of the dopant ion. The obtained suspension was stirred for 30 min at 60 °C, then 0.36 mol of ethanol and 0.10 mol of reaction catalyst (HCl, HNO<sub>3</sub> and 0.05 mol in the case of H<sub>2</sub>SO<sub>4</sub>) were added to the solution which was left under rapid stirring for a fixed time length (120 min, first hydrolysis). Subsequently Zr(OC<sub>3</sub>H<sub>7</sub>)<sub>4</sub> (0.20 mol) was added drop by drop to the suspension and finally the last 260 ml of milli-Q water were mixed. The final suspension was kept under stirring at 60 °C for fixed time length (30 min, second hydrolysis). The homogeneous wet gel, cooled at room temperature, was dried in oven at 60 °C (xerogel) and then was thermally treated in the temperature range of 800–1300 °C.

The samples have been denoted as following:

- the first letter is relative to the anionic environment and the anionic partner of iron (C = chloride, N = nitrate, S = sulphate);
- the doped samples with different iron content (%Fe<sub>2</sub>O<sub>3</sub>/Zr), for example, 0.7%, 4.5%, 5%, 10%, in chloride environment are denoted C007, C045, C050, C100.

### 2.2. Sample characterisation

Structural characterisation of the powders was performed by X-ray diffraction, using a Siemens D500 diffractometer, using Cu K $\alpha$  radiation in the 10–80° 2 $\theta$  angle range. The fitting program of the peaks was a particular Rietveld program,<sup>15,16</sup> named QUANTO,<sup>17</sup> devoted to the automatic estimation of the weight fraction of each crystalline phase in a mixture.

The peak shape was fitted using a modified Pearson VII function. The background of each profile was modelled using a six-parameters polynomial in 2 $\theta^m$ , where  $m$  is a value from 0 to 5 with six refined coefficients.

The mean dimension,  $d$ , of crystallites was obtained by elaborating the most intense X-ray peak of each phase by

the Scherrer's equation:

$$d = \frac{K\lambda}{\beta \cos \theta}$$

where  $K$  is a constant related to the crystallite shape (0.9),  $\beta$  is the pure breadth of the powder reflection, free of the broadening due to the instrumental contributions. This calibration was performed by means of the spectrum of a standard Si powder. The accuracy with which the Scherrer's equation can be applied is limited by the uncertainties in  $K$  and by the success with which  $\beta$  can be deduced from the experimentally observed breadth. This equation is quite satisfactory for studies comparing the crystallite sizes of a number of samples belonging to a related series.

SEM-EDX analyses were performed using a Hitachi 2400 scanning electronic microscope equipped with a quantum Kevex energy-dispersive X-ray micro-analyser (EDX). Powder samples were coated with a thin gold layer deposited by means of a sputter coater.

Diffuse reflectance spectra were acquired in the Vis-NIR range from 350 to 1200 nm using a JASCO/UV/Vis/NIR spectrophotometer model V-570 equipped with a barium sulphate integrating sphere. A block of mylar was used as reference sample following a previously reported procedure.<sup>18</sup>

The colour of the fired samples was assessed on the grounds of  $L^*$ ,  $a^*$  and  $b^*$  parameters, calculated from the diffuse reflectance spectra, through the method recommended by the Commission Internationale de l'Eclairage (CIE).<sup>19</sup> By this method the parameter  $L^*$  represents the brightness of a sample; a positive  $L^*$  value stays for a light colour while a negative one corresponds to a dark colour;  $a^*$  represents the green (–) → red (+) axis and  $b^*$  the blue (–) → yellow (+) axis.

### 3. Results and discussion

#### 3.1. Structural and textural characterisations

Fig. 1 reports the X-ray pattern of three samples, calcined respectively at 800, 1000 and 1200 °C, prepared in chloride environment with the same 0.05 Fe<sub>2</sub>O<sub>3</sub>/Zr molar ratio. It can be observed that the tetragonal zirconia polymorph is the sole crystalline phase at 800 °C; at 1000 °C the peaks of zircon are appreciable, together with the ones of monoclinic zirconia but the tetragonal component is still the major one. At 1200 °C, instead, zircon is present as the main component together with monoclinic zirconia; tetragonal zirconia, hematite (α-Fe<sub>2</sub>O<sub>3</sub>) and cristobalite (SiO<sub>2</sub>) although in traces, are appreciable in the spectrum. These results are in agreement with literature data which describe the nucleation of the zircon structure to be supported by the presence of the metal dopant within the tetragonal zirconia lattice.<sup>6,11,12</sup>

In order to obtain an accurate quantitative estimation of the fraction of zircon phase present in the powders, the spectra of three samples, obtained with different starting iron

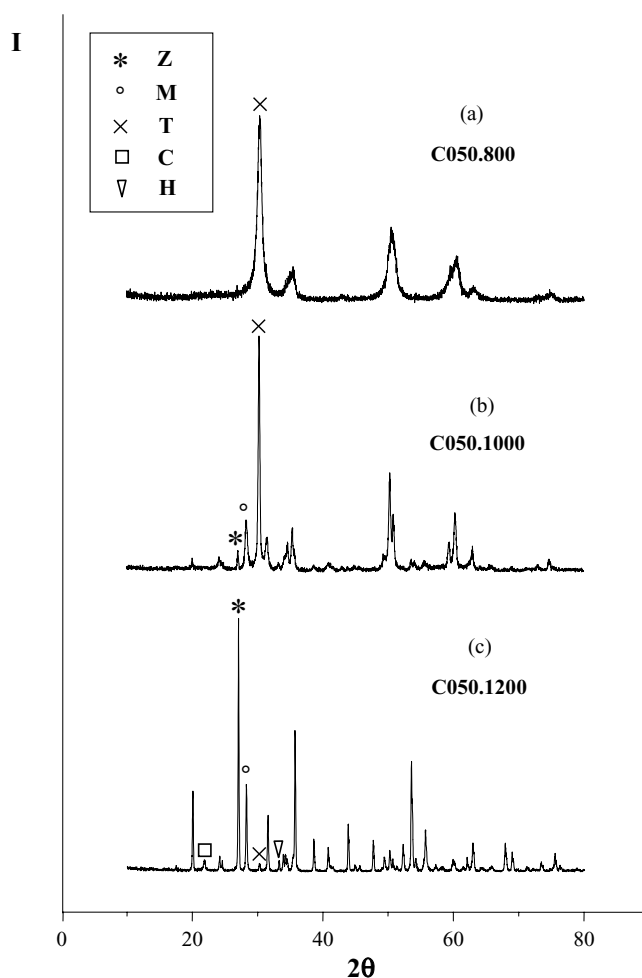


Fig. 1. Powder X-ray diffraction spectra of doped samples (5% Fe<sub>2</sub>O<sub>3</sub>/Zr) in chloride environment calcined at different temperatures: (a) 800 °C, (b) 1000 °C, (c) 1200 °C.

content and calcined at 1000, 1200 and 1300 °C have been fitted with the Rietveld program QUANTO; the results are reported in Table 1. As a general trend, the amount of zircon phase can be observed to increase, for each iron content, with the temperature of calcination. The formation of

Table 1  
Main crystalline phases of all samples as a function of the calcination temperature

Sample	wt.% (Z)	wt.% (M)	wt.% (T)	wt.% (C)	wt.% (H)
C007.1000	–	1.5	98.5	–	–
C007.1200	51.8	24.2	7.0	17.0	–
C007.1300	64.7	22.4	2.0	10.9	–
C050.1000	4.8	30.2	60.3	0.7	4.0
C050.1200	60.6	20.8	2.2	11.8	4.6
C050.1300	68.4	17.8	1.4	7.7	4.7
C100.1000	–	13.5	75.6	3.7	7.2
C100.1200	51.4	25.9	2.6	11.6	8.5
C100.1300	54.9	27.2	1.0	8.1	8.8

M: ZrO<sub>2</sub> (monoclinic), T: ZrO<sub>2</sub> (tetragonal), Z: ZrSiO<sub>4</sub> (zircon), C: SiO<sub>2</sub> (cristobalite), H: α-Fe<sub>2</sub>O<sub>3</sub> (hematite).

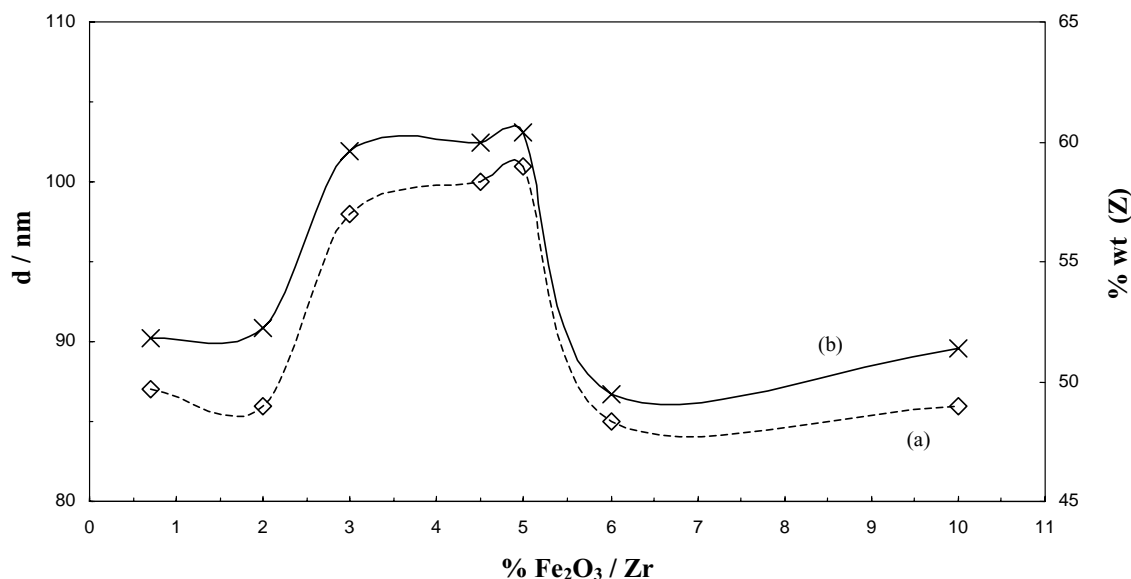


Fig. 2. (a and b) Structural features of 1200 °C calcined samples in chloride environment at variable Fe<sub>2</sub>O<sub>3</sub>/Zr molar ratios. Quantitative phase composition by the QUANTO elaboration of X-ray diffractograms; Crystallite sizes by Scherrer's equation.

zircon, seemingly, occurs at the expenses of tetragonal zirconia, whose amount decreases markedly with the temperature. Crystobalite is present in traces at 1000 °C as SiO<sub>2</sub> is still mainly amorphous at this temperature; as the crystallization of zircon proceeds the crystalline amount of crystobalite decreases. The presence of crystalline hematite, not appreciable for the lowest iron content, increases with the initial starting amount of iron and the temperature of calcination.

The singular aspect which emerges from the analysis of data in Table 1 is the appearance, at 1000 °C, of the zircon phase only for the intermediate iron concentration (5%) and that for each temperature the 5% iron content provokes the formation of the largest zircon amount.

In order to investigate, in detail, the role played by the iron content on both the zircon promotion and the size of the crystallites, samples with variable Fe<sub>2</sub>O<sub>3</sub>/Zr starting ratios were analyzed. Fig. 2 shows that the amount of zircon phase is not a simple function of the iron concentration in the starting mixture but goes through a maximum (up to around 60%) for iron molar ratios in the range 3–5% and then it levels off to lower contents. Also the size of the crystallites shows a very similar trend with varying the iron amount; the conditions of best promotion of the zircon phase are matched by the largest crystallite sizes. On the grounds of the generally reported role of iron on the formation of the zircon structure a promoting effect increasing regularly with the starting iron content could have been expected. To this end it is worth reporting that in the present case no effects of distortion of the tetragonal lattice have been observed for any iron content. The parameters of the unit cell of the tetragonal phase at 800 °C have been found in fact to be invariant with the starting iron content.

The role played by the amount of iron in the sample is evidenced also by EDX analyses obtained for samples with variable Fe<sub>2</sub>O<sub>3</sub>/Zr molar ratios (Fig. 3). All samples, even after calcination at 1200 °C, are composed by several crystalline and amorphous phases (ZrSiO<sub>4</sub>, ZrO<sub>2</sub>, SiO<sub>2</sub>, Fe<sub>2</sub>O<sub>3</sub>), as shown by data in Fig. 1 and Table 1. EDX data show in fact that different regions of the same sample are differently enriched in the various phases. For iron contents lower or equal to 5%, the iron peak is appreciable only when the amount of Zr-containing compounds is larger than that of Si (Fig. 3a<sub>1</sub>, a<sub>2</sub>). This result suggests that iron is preferably located either in ZrSiO<sub>4</sub> or in ZrO<sub>2</sub> and less (or nihil) in SiO<sub>2</sub>, either crystalline or amorphous. For iron oxide contents larger than 5%, instead, the amount of iron is found to vary significantly in the different positions of the same sample, independently of the Zr/Si local amounts (see e.g. Fig. 3b<sub>1</sub> and b<sub>2</sub>). This finding suggests that for higher Fe concentrations hematite is present in the samples as a separate phase not only distributed (either encapsulated or as interstitial Fe species) in the Zr-containing lattices.

The promotion of the zircon structure and the growth of the crystallites are primarily defined by the starting iron content in the preparative mixture (e.g. Fig. 2). However also the speciation of the anionic partner of iron (and of the acid catalyst) can provoke appreciable effects, as we have previously observed.<sup>14</sup> Fig. 4 shows that, in the case of 5% Fe<sub>2</sub>O<sub>3</sub>/Zr, both the formation of the zircon phase and the size of the crystallites are at the maximum when the anions are chlorides while they drop to much lower values in the case of sulphates. Among the three different anions (Cl<sup>−</sup>, NO<sub>3</sub><sup>−</sup>, SO<sub>4</sub><sup>2−</sup>), chloride ions, which are small and only physically interacting with oxides show a promoting role, while the strong chemical interactions present in the case of

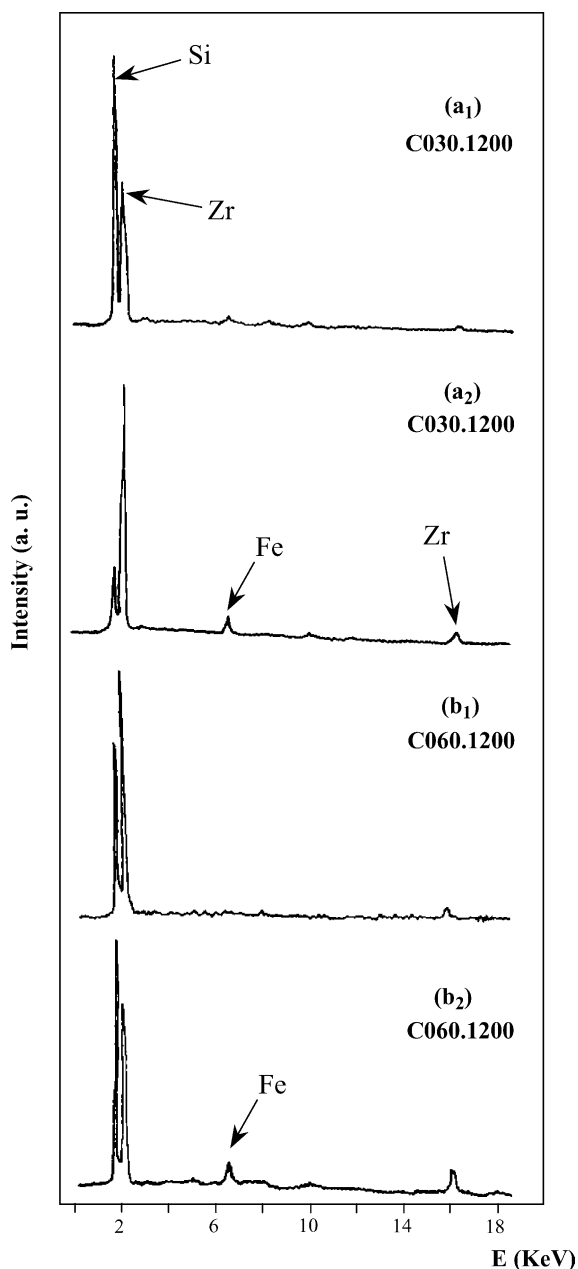


Fig. 3. EDX analyses of 1200 °C calcined samples in chloride environment (a<sub>1</sub>) and (a<sub>2</sub>) different regions of C030; (b<sub>1</sub>) and (b<sub>2</sub>) different regions of C060. The EDX spectra are acquired on samples area of 200 μm × 200 μm using a magnification of 500×.

sulphates lead to the formation of xerogels which evolve to lower zircon content and smaller crystallite sizes. The anion size, hydration and interacting capability apparently impose the features of the tridimensional gel network, in its turn affecting the silicon nucleating step leading to the zircon phase.

### 3.2. Diffuse reflectance characterisations

Diffuse reflectance spectra have been acquired on the samples calcined at 1200 °C. In all the spectra the presence of

hematite signals has been disclosed as it is possible to observe in Fig. 5 where, as an example, the spectra acquired on samples C007, C050 and C100 are reported together with hematite spectra. Hematite is characterised by absorption signals at 500, 660 and 860 nm, which are typical of this phase.<sup>14,15</sup> The higher wavelength peaks (660, 860 nm) are appreciable also in the spectra of the iron-doped zircon samples while the presence of a large absorption signal below 500 nm could hide the third hematite absorption peak at 500 nm. Therefore the origin of the red colour of the zircon powders is, at least in part, to be attributed to the presence of hematite in the samples, as generally reported in the literature.<sup>6,8</sup> Furthermore, examining the second derivatives spectra (not shown), the presence of interstitial iron located in the octahedral positions of the zircon lattice has been put in evidence in all the samples at 470 and 565 nm. The concomitant presence of hematite and interstitial ions located in octahedral positions was already observed by us in a previous work.<sup>14</sup>

From the diffuse reflectance spectra  $L^*$ ,  $a^*$  and  $b^*$  parameters have been calculated. The obtained data are reported in Table 2 together with the values determined, by us, for hematite; the table reports also, for the sake of comparison, the parameters of literature pigments,<sup>6</sup> prepared respectively by a ball milling (CER) and a colloidal procedure (CC). By comparing the parameters of the present samples with the ones of pure hematite, it can be seen that, going from sample C007 to hematite the  $L^*$  parameter decreases indicating a progressively more intense colour. The values of  $a^*$  and  $b^*$  parameters, instead, do not show a definite trend with the iron content. The CER sample, obtained by a classic ceramic procedure, shows with respect to the present samples a more intense coral hue, i.e. a much higher value of  $a^*$  which is the parameter representative of the red colour and a lower  $L^*$  value which indicates a darker and more intense colour. The pigments obtained in the present study by sol-gel procedure have a pink hue and are more similar to CC, a pink sample synthesised by Monros and co-workers<sup>6</sup> through a colloidal procedure. In comparison with this latter sample our pigments show lower values for the  $b^*$  parameter indicating that their colour is less affected by yellow shades.

Table 2  
CIE  $L^*a^*b^*$  parameters of Fe pigments samples, calcined at 1200 °C

Sample	$L^*$	$a^*$	$b^*$
C007	76.0	14.5	14.6
C020	68.5	15.3	11.2
C030	67.3	14.1	10.2
C045	64.3	17.8	12.9
C050	62.7	12.6	7.6
C060	58.5	15.7	10.7
C100	54.4	14.3	8.9
Hematite	50.0	10.8	2.8
CER <sup>6</sup>	55.7	29.5	24.2
CC <sup>6</sup>	70.3	17.8	26.6

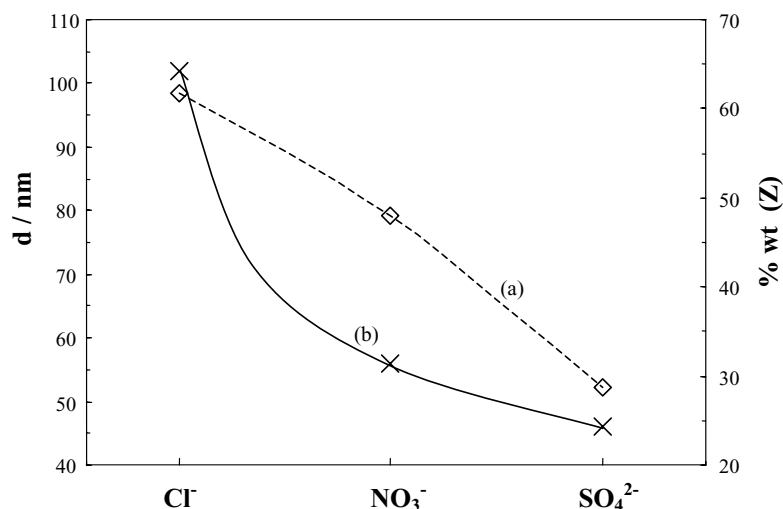


Fig. 4. Structural features of C050 calcined at 1200 °C as a function of the different anionic environment. Quantitative phase composition by the QUANTO elaboration of X-ray diffractograms. Crystallite sizes by Scherrer's equation.

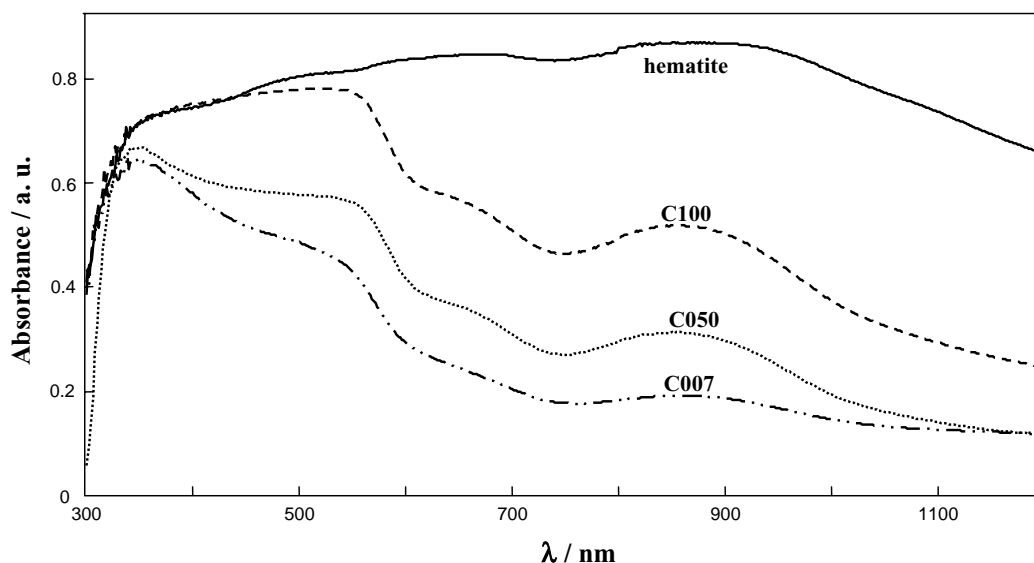


Fig. 5. Diffuse reflectance spectra for samples C007, C050 and C100 calcined at 1200 °C and pure hematite, in the range from 1200 to 300 nm.

#### 4. Conclusions

ZrSiO<sub>4</sub> precursors containing increasing iron oxide starting amounts (in the range 0.7–10% molar ratio) were obtained by a sol–gel reaction, in water-ethanol mixtures, at 60 °C. All the precursors were calcined from 800 to 1300 °C.

Structurally, intermediate (5%) iron oxide contents were found to provoke singular effects with respect to both higher and lower metal concentrations: (i) zircon started to form at lower temperatures; (ii) the size of the crystallites was larger; (iii) the relative phase enrichment in both zircon and monoclinic zirconia was favoured with respect to the tetragonal phase.

Diffuse reflectance analyses showed that the colour of the pigments was the result of both hematite and interstitial

iron. The colour hue was pink, free of yellow shades, and became more intense with increasing the iron content of the sample.

#### Acknowledgements

Financial support from the Ministry of Education, University and Research (MIUR, FIRST Funds) is gratefully acknowledged.

#### References

1. Eppler, R. A., Resistance of porcelain enamels to attack by aqueous media. II. Equations to predict enamel durability. *J. Am. Ceram. Soc.* 1979, **53**, 457.



2. Gair, I., Jones, R. H., Airey, A. C., Sankar, G. and Gleeson, D., *Communication Presented in the VI World Congress on the Quality of Wall and Floor Ceramics Tiles (QUALICER), Castellon (Spain), March 2000.*
3. Tartaj, P., Serna, C. J., Soria, J. and Ocana, M., Origin of color in aerosol-derived vanadium-doped zirconia pigments. *J. Mater. Res.* 1998, **13**, 413.
4. Ocana, M., Caballero, A., Gonzalez-Elipe, A. R., Tartaj, P., Serna, C. J. and Merino, R. I., The effects of the NaF flux on the oxidation state and localization of praseodymium in Pr-doped zircon pigments. *J. Eur. Ceram. Soc.* 1999, **19**, 641.
5. Tartaj, P., Gonzalez-Carreno, T., Serna, C. J. and Ocana, M., Iron zircon pigments prepared by pyrolysis of aerosols. *J. Solid State Chem.* 1997, **128**, 102.
6. Llusar, M., Calbo, J., Badenes, J. A., Tena, M. A. and Monros, G., Synthesis of iron zircon coral by coprecipitation routes. *J. Mater. Sci.* 2001, **36**, 153.
7. Berry, F. J., Eadon, D., Holloway, J. and Smart, L. E., Iron-doped zirconium silicate. Part 1. The location of iron. *J. Mater. Chem.* 1996, **6**(2), 221.
8. Berry, F. J., Eadon, D., Holloway, J. and Smart, L. E., Iron-doped zircon: the mechanism of formation. *J. Mater. Sci.* 1999, **34**, 3631.
9. Carreto, E., Pina, C., Arriola, H., Barahona, C. A., Nava, N. and Castano, V., Mossbauer study of the structure of Fe-zircon system. *J. Radioanal. Nucl. Chem.* 2001, **250**, 453.
10. Airey, A. C. and Roberts, W., Advances in ceramic colors. *Ceram. Eng. Sci. Proc.* 1987, **8**, 1168.
11. Llusar, M., Badenes, J. A., Calbo, J., Tena, M. A. and Monros, G., Environmental and colour optimisation of mineraliser addition in synthesis of iron zircon ceramic pigment. *Br. Ceram. Trans.* 2000, **99**, 14.
12. Eppler, R. A., Kinetics of formation of an iron-zircon pink color. *J. Am. Ceram. Soc.* 1979, **62**, 47.
13. Li, C. and Eppler, R. A., Iron zircon pigments. *Ceram. Eng. Sci. Proc.* 1992, **13**, 109.
14. Ardizzone, S., Binaghi, L., Cappelletti, G., Fermo, P. and Gilardoni, S., Iron doped zirconium silicate prepared by a sol-gel procedure. The effect of the reaction conditions on the structure, morphology and optical properties of the powders. *Phys. Chem. Chem. Phys.* 2002, **4**, 5683.
15. McCusker, L. B., Von Dreele, R. B., Cox, D. E., Louer, D. and Scardi, P., Rietveld refinement guidelines. *J. Appl. Crystallogr.* 1999, **32**(1), 36.
16. Hill, R. J. and Howard, C. J., Quantitative phase analysis from neutron powder diffraction data using the Rietveld method. *J. Appl. Crystallogr.* 1987, **20**(6), 467.
17. Altomare, A., Burla, M. C., Giacovazzo, C., Guagliardi, A., Moliterni, A. G. G., Polidori, G. et al., Quanto: a Rietveld program for quantitative phase analysis of polycrystalline mixtures. *J. Appl. Crystallogr.* 2001, **34**(3), 392.
18. Borgia, I., Brunetti, B., Mariani, I., Sgamellotti, A., Cariati, F., Fermo, P. et al., Heterogeneous distribution of metal nanocrystals in glazes of historical pottery. *Appl. Surf. Sci.* 2002, **185**(3/4), 206.
19. CIE, *Recommendations on Uniform Colour Spaces, Colour Difference Equations, Psychometrics Colour Terms*. Supplement No. 2 of CIE Publ. No. 15 (E1-1.31) 1971. Bureau Central de la CIE, Paris, 1978.